

Nucleation of Ge dots on the C-alloyed Si(001) surface

O. Leifeld,^{1,2,*} A. Beyer,² D. Grützmacher,² and K. Kern^{1,3}

¹Max-Planck-Institut für Festkörperforschung, Heisenbergstrasse 1, D-70569 Stuttgart, Germany

²Laboratory for Micro- and Nanotechnology, Paul Scherrer Institut, CH-5232 Villigen-PSI, Switzerland

³Institut de Physique des Nanostructures, EPFL, CH-1015 Lausanne, Switzerland

(Received 25 June 2002; published 26 September 2002)

The growth of Ge on Si(001) surfaces precovered with 0.1 ML carbon has been investigated by ultrahigh vacuum scanning-tunneling microscopy. Unlike the Stranski-Krastanov growth of Ge on bare Si(001), three-dimensional islands start to nucleate already at submonolayer Ge coverage. This Volmer-Weber growth mode is forced by the surface strain pattern related to the C incorporation into the Si surface. Ge dots nucleate between the $c(4\times 4)$ reconstructed C-rich areas, where the lattice mismatch is higher with respect to Ge. Based on this observation and the evolution of islands towards higher Ge coverage, which give insight into the spatial dot composition, a modified model for the photoluminescence mechanism of C-induced Ge dots is proposed.

DOI: 10.1103/PhysRevB.66.125312

PACS number(s): 68.35.Dv, 68.37.Ef, 68.55.Jk, 73.21.La

Remarkably small Ge quantum dots can be fabricated by molecular-beam epitaxy when Ge is deposited onto a Si(001) surface precovered with a small fraction of a monolayer of carbon.^{1,2} These dots occur below the critical thickness of the usual Stranski-Krastanov growth mode of Ge on bare Si(001). Such carbon-induced Ge dots (GeC dots) have been shown to exhibit strong photoluminescence. Obviously, both the early three-dimensional growth and the photoluminescence (PL) properties are related to the carbon involved in the structures. Some effort has been undertaken to study the PL behavior of GeC dots. However, the atomic composition within the GeC islands was not known, since so far no *in situ* observation of the dot-formation process has been done, making it difficult to interpret PL data.

Starting from the knowledge of the C-alloyed Si(001) surface structure, which has been determined in an earlier work by ultrahigh vacuum scanning-tunneling microscopy (UHV STM) and density-functional calculations,³ in this paper the initial stages of Ge nucleation and island growth on this surface at different growth temperatures are unraveled by UHV STM. The molecular-beam epitaxy system used for the sample preparation has two electron-beam evaporators for Si and Ge and a carbon sublimation source, which is essentially a well-shielded pyrolytic graphite filament heated by direct current flow. Samples always consist of complete 4-in. wafers that are chemically cleaned and hydrogen passivated before being loaded into the vacuum system. After an annealing of the wafer to 950 °C for oxide desorption a 100-nm-thick Si buffer layer is grown at 750 °C. The wafer is allowed to cool down to a temperature of 530 °C, at which the 0.1 ML of C is deposited at a rate of 3.3×10^{11} at./s. Under these conditions the surface forms the $c(4\times 4)$ reconstructed superstructure due to C incorporation. Subsequently the temperature is lowered to the deposition temperature for Ge. Ge is evaporated at a rate of (0.01 ± 0.01) ML/s for the coverages up to 1 ML, and at a ten times faster rate for higher coverage. After completion of the sample, the 4-in. wafer is allowed to cool down to room temperature and immediately transferred to the STM chamber⁴ while maintaining UHV conditions.

The choice of suitable substrate temperatures for the observation of Ge nucleation with STM has been lead by different considerations. When growing Ge at substrate temperatures above 500 °C on bare Si(001), intermixing of Ge adatoms with the Si substrate within the first monolayer is usually observed.⁵ So the identification of single Ge atoms with STM is obstructed, since to date it has not been possible to distinguish (even with spectroscopic STM techniques) between alloyed Si and Ge atoms at the surface. A distinction between the species is only possible when Ge forms a different surface texture than the substrate, like a reconstruction or islands. On Si(001), however, Si and Ge have the same (2×1) reconstruction.

When Ge grows on bare Si(001) without C at a temperature of 350 °C, intermixing is negligible and the growth is kinetically limited by diffusion on the Si(001) surface, leading to elongated two-dimensional Ge islands due to the diffusion anisotropy on the Si(001) terraces.⁶ So the nucleation experiments of Ge on the 0.1 ML C / Si(001) surface have also been performed at this temperature. The same experiments have been repeated at 530 °C to be able to compare the submonolayer growth with the samples containing several monolayers of Ge, that show intense PL signals.

Figure 1 shows a series of Ge coverages (0.1, 0.5, and 1 ML) deposited at 350 °C onto the 0.11 ML C / Si(001) substrate. Already at 0.1 ML Ge [Fig. 1(a)] a number of small single-layer Ge islands have nucleated on terraces (indicated by arrows), each surrounded by buckled dimer rows in the terrace layer, which are assumed to be silicon. Compared to the more elongated islands reported on bare Si(001), the island aspect ratio is small. Diffusion anisotropy on the surface seems to be reduced due to the presence of the $c(4\times 4)$ regions. Ge adlayer islands are not found directly on top of a $c(4\times 4)$ area. An island density of $(8\pm 1)\times 10^{11}$ cm⁻² is determined at this coverage. If all Ge adatoms were contained in the islands, these would have an average size of 8×11 at. In fact the measured islands are smaller, implying that a substantial amount of Ge ($\sim 50\%$) is incorporated at step edges. Presumably it is energetically favorable for Ge atoms impinging onto a $c(4\times 4)$ domain near an S_B step to

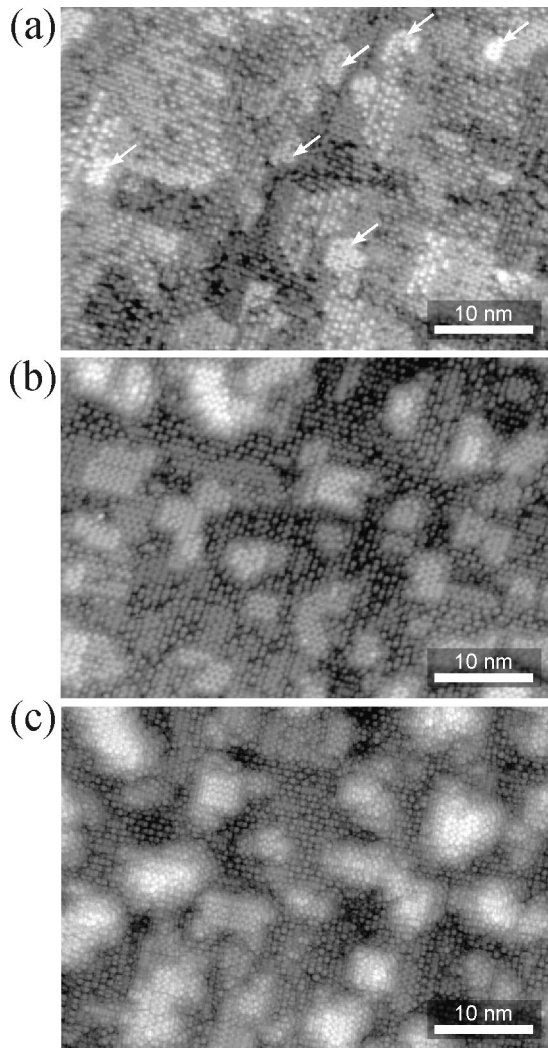


FIG. 1. Series of STM images of different Ge coverages deposited onto 0.11 ML C / Si(001) at a substrate temperature of 350 °C and a flux of 0.01 ML/s. Image size is 35 nm \times 50 nm each. (a) 0.1 ML Ge; arrows mark small single-layer Ge islands on the terraces (-2 V, 0.17 nA). (b) 0.5 ML Ge; (-2.3 V, 0.2 nA) 3D islands pile up to 3–4 ML, and $c(4\times 4)$ regions remain in between islands. (c) 1 ML Ge; (-2.4 V, 0.2 nA) islands have increased in height and size compared to (b).

leave it by migrating down a step in places where the lower terrace is (2×1) reconstructed.

The observation that the Ge atoms do not nucleate on the C-rich $c(4\times 4)$ reconstruction agrees well with the predicted repulsive interaction of Ge and C in this SiGeC material system.⁷ Considering bond lengths and lattice constants, this is plausible: in the $c(4\times 4)$ areas the Si surface is compressively strained due to the high carbon content, reducing the average lattice constant here. Furthermore, C is present directly at the surface. Both facts discourage the larger Ge atoms from nucleating in these areas, since the formation of Ge-C bonds would involve severe amounts of strain due to the difference in bond length of -37% . Instead, the Ge tends to wet the $\text{Si}(2\times 1)$ regions first, since they are even under tensile stress between the C-containing areas. The re-

sulting lattice mismatch of less than 4% favors Ge nucleation on the $\text{Si}(2\times 1)$ areas.

Increasing the Ge coverage to 0.5 ML, the island density is only slightly augmented to a value of $(9.5\pm 1.0)\times 10^{11}$ cm $^{-2}$. The rms roughness rises by 50% simultaneously. Consequently the islands grow in size and height, being laterally restricted by the $c(4\times 4)$ areas. Still, the Ge atoms seem to avoid the formation of Ge-C bonds and therefore start nucleating on top of the existing islands, resulting in 3D island growth [Fig. 1(b)]. The restructuring of the Si surface due to the C predeposition obviously forces Ge to grow in a Volmer-Weber mode rather than a Stranski-Krastanov mode at the given temperature. The area between the islands is mainly $c(4\times 4)$ reconstructed. Islands have most frequently a rectangular shape of a low aspect ratio with their edges aligned along $\langle 110 \rangle$.

Interestingly most of the 3D islands are located at step edges, forming the border between adjacent terraces in those places, where the $c(4\times 4)$ reconstruction does not reach a step. The highest islands are found at S_B step segments, whereas islands in terrace centers remain smaller and flatter. The explanation could be that Ge adatoms migrate on the upper terrace along dimer rows towards the step, descend, and are incorporated there, corresponding to the initial stages of a step flow mode. But the lateral extension of this first monolayer of an island is restricted when it approaches the $c(4\times 4)$ regions on the lower terrace, because of the reluctance to form Ge-C bonds. Instead, the Ge atoms start to pile up three dimensionally, preferentially nucleating on top of the existing Ge areas, where the difference in lattice constants is smallest. Consequently, this 3D growth is driven by strain relaxation, because the C-enriched Si surface areas have a smaller average lattice constant.

The evolution of the 3D islands outlined above continues towards higher Ge coverage. At 1 ML Ge deposited at 350 °C the Ge still does not cover the whole surface but instead keeps growing as 3D piles. Therefore, the rms roughness increases further, while the island density slightly decreases to $(8\pm 1)\times 10^{11}$ cm $^{-2}$. Island diameters increase to 4–5 nm, the height increases, and the size distribution slightly broadens. In areas between the islands the unperturbed $c(4\times 4)$ reconstruction is still completely visible. Figure 1(c) shows the surface morphology for 1 ML Ge coverage.

It is remarkable that the shape of the basis of the higher islands becomes more irregular with respect to 0.5 ML, where the rectangular shape dominates. More rounded shapes are now also found and the longer axes of many islands deviate from the $\langle 110 \rangle$ direction. The reason may be the coalescence of neighboring islands. It is difficult to determine the side facets of these relatively small islands. No distinct facet reconstruction can be seen because sidewalls are irregular. Nevertheless, a certain affinity to side facet formation either in $\langle 100 \rangle$ or $\langle 110 \rangle$ directions is visible in the images. Most likely the facets are made up from close trains of S_A and rebounded S_B steps along $\langle 110 \rangle$ and (104) facets along $\langle 100 \rangle$, having inclination angles of $\sim 11^\circ$ to $\sim 15^\circ$ with respect to the (001) surface.

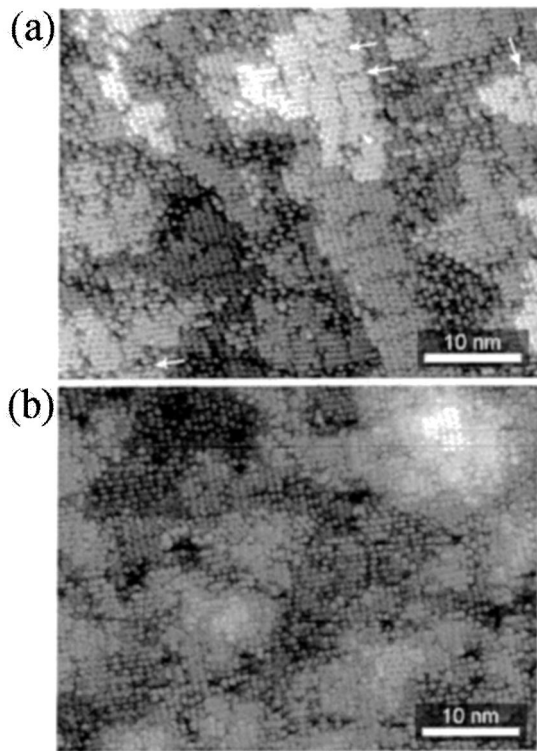


FIG. 2. (a) 0.5 ML and (b) 1 ML Ge deposited onto 0.11 ML C/Si(001) at a substrate temperature of 530 °C.

We point out that up to this coverage no Ge wetting layer is formed. Instead, the area between 3D islands is made up exclusively of the C-rich $\text{Si}_{1-x}\text{C}_x$ alloy. We assume that virtually no Ge incorporates into the $c(4\times 4)$ regions, since this would almost certainly alter the appearance of these regions in the STM images. The reason for this is, as explained above, the repulsive interaction between Ge and C, which is a result of the large local strains that would be associated with such a mixture.⁷

So far it has been demonstrated that at a substrate temperature of 350 °C, Ge is completely repelled by the C-rich areas on 0.11 ML C / Si(001) surfaces and grows three dimensionally. For thicker Ge films, such as of 2.5 ML and more, grown at 530 °C the $c(4\times 4)$ reconstructed areas have disappeared and only larger 3D islands are found.⁸ For this reason we assume intermixing of Ge with the $\text{Si}_{1-x}\text{C}_x$ areas at this temperature and coverage. To uncover the intermixing process and island formation at 530 °C the evolution of Ge growth below one monolayer is further investigated.

In Fig. 2(a) a 50 nm \times 35 nm STM image of 0.5 ML Ge on 0.11 ML C / Si(001) is shown. It gives the impression of a step flow dominated growth. For the C precovered surface it has been shown that the $c(4\times 4)$ areas are preferentially formed at step edges. So these are usually terminated by a $c(4\times 4)$ pattern. After the deposition of 0.5 ML Ge, the areas around steps are mostly (2×1) reconstructed. Therefore they are expected to consist of Ge indicated by the characteristic missing dimer superstructure. In contrast to the S_A steps, the S_B steps are still often formed by $c(4\times 4)$ rows. In general one still finds a lot of $c(4\times 4)$ areas, demonstrating the repulsion of Ge by the C-rich areas even at this substrate

temperature of 530 °C. However, intermixing between Ge and C is probably not negligible, since some of the (2×1) reconstructed areas contain—in addition to the strain-relieving perpendicular missing dimer rows—rows with a periodic train of missing dimer defects [indicated by arrows in Fig. 2(a)]. In these rows only every third or fourth dimer is visible, a structure not usually observed in Ge or SiGe adlayers. Yet the growth does not proceed purely in step flow mode, since the second layer has nucleated on top of many islands. Islands with extensions of about 20 nm are dominant, having rather an isotropic shape. On all of them the Ge missing dimer rows are developed. Large islands exist predominantly in the vicinity of steps. Nucleation of a third layer on top of the large islands is rarely observed, indicating that the diffusion length of Ge adatoms on these large islands is higher than the island diameter and the activation barrier for diffusing down the island edges is overcome at this growth temperature. Different diffusion lengths on terraces and on islands may be responsible for this effect. If they were identical one should find pure step flow growth. Hence, intuitively one can conclude that the presence of the C-rich $c(4\times 4)$ hampers the diffusion on the terraces.

The island density at this surface is $(3\pm 1)\times 10^{11}\text{ cm}^{-2}$. This value is only a factor of 3 lower compared to the island density at 350 °C. For the temperature difference of 200 K this difference in island density is remarkably small. From Si (Ref. 9) or Ge nucleation on bare Si(001) surfaces one expects a drop of the island density by several orders of magnitude, because diffusion is a thermally activated process.¹⁰ Again, it is the presence of the C-rich $c(4\times 4)$ reconstructed areas and their repulsive interaction with the Ge which modifies the fundamental growth process.

As already pointed out in the beginning of this paper a certain amount of intermixing between Ge and the Si within the first monolayer is expected at 530 °C. It was predicted to be below 25%.⁵ Thus the (2×1) dimer-reconstructed areas in the substrate layer and the first monolayer are most probably a $\text{Si}_{1-x}\text{Ge}_x$ alloy. This alloy is Si rich in the substrate layer and Ge rich in the first adlayer. The second layer consists almost exclusively of Ge.

Figure 2(b) shows an STM image of the surface after one-monolayer Ge deposition at 530 °C. Note the surface still exhibits substantial amounts of $c(4\times 4)$ reconstructed areas. Even at 530 °C the Ge does not wet the whole surface but is still essentially repelled by the C-rich areas. The island growth is more pronounced for monolayer coverage than for 0.5 ML and the roughness has increased by 70%. Some islands have a height up to 6 ML. The largest islands have sizes of 10 to 15 nm. The majority of them, however, are flat, rarely exceeding a height of three monolayers. The island density remains constant at a value of $(3\pm 1)\times 10^{11}\text{ cm}^{-2}$. The large islands are expected to grow on top of the large two-layer-high islands found at 0.5 ML, whereas the smaller islands do not pile up further. This is reasonable since the growth of the smaller islands, which is laterally restricted by the strain in surrounding areas, would lead to steeper sides, which is unfavorable in terms of surface energy. Furthermore, the supply of the small islands with adatoms is kinetically restricted since they have a smaller capture area.

Intermixing of Si and Ge depends primarily on the substrate temperature, but as for any thermodynamic mixing (diffusion) process the particle density is involved, too. Therefore at higher Ge coverage intermixing is expected to become more important. Consequently the $c(4 \times 4)$ areas become more disordered compared to the situation with a coverage of 0.5 ML Ge. In some places the same unusual rows with periodically missing dimers are found as is the case for 0.5 ML Ge. This could be interpreted as a sign for a partial intermixing of Ge and Si in C-rich areas.

The observation of the preferential Ge island nucleation on the C-free areas gives insight into the spatial material composition of the C-induced Ge quantum dots at higher Ge coverage, which were found to show improved photoluminescence (PL).^{11,12} In the picture of Ref. 11 such dots are described as having a gradual composition profile from homogeneous SiGeC at the bottom to pure Ge towards their apex. This would also lead to a gradual transition of the band alignment within each dot from a type-I confinement of electrons in the conduction band in the C-rich lower SiCGe region towards a confinement of heavy holes in the valence band at the Ge-rich dot apex. Hence the optical transition involves a type-II recombination of the electron-hole pairs confined in different regions of the dots. This is possible, since Bohr radii of bound excitons in SiGe can be as large as 11 nm,¹³ and thus are typically larger than the height of ≤ 3 nm of these small islands. A schematic drawing of the dot composition and the bands assumed in this model is given in Fig. 3(a).

However, our results concerning the submonolayer dot nucleation point to a different model for the recombination mechanism. At 2.5–3 Ge ML, for instance, irregular Ge dots with a density of $\sim 1 \times 10^{11} \text{ cm}^{-2}$ and sizes around 10–20 nm have been reported at the same growth conditions.¹ These dots evolve from the small 3D dots by further growth and coalescence and a gradual intermixing or coverage of the C-rich areas with Ge. Considering the strain as the basic driving force for the submonolayer dot formation, it is evident that even these larger dots are still centered above locations free of C. Their edges extend over the C-rich SiC areas. An idealized scheme of the spatial material composition based on these observations is given in Fig. 3(b). Dots free of C with a gradual composition profile from SiGe at the bottom to Ge at the apex are located between C-rich SiC

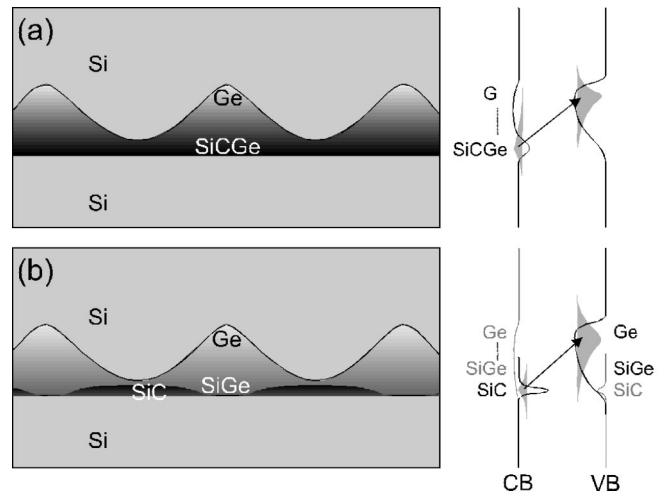


FIG. 3. Scheme of spatial dot compositions and the related band structure. The spatially indirect recombination paths are indicated. (a) is taken from Ref. 11 and (b) is derived from the present nucleation and growth experiments.

patches. Hence, there potentially is a strong confinement of electrons in the SiC, whereas holes would be exclusively trapped in the islands. Then, following the same arguments as in the first case, the spatially indirect recombination of the carriers from the island position to the SiC regions is possible when their distance is smaller than the exciton binding radius. This is strongly favored, when the islands are small and their density is high.

This model can also explain why the PL intensity rapidly goes down with increasing Ge coverage, as reported in Ref. 12, where it is maximum for 2.5 ML Ge and nearly vanishes for 4 ML Ge. The increasing Ge overlayer thickness leads in this model to an increase of the Ge layer above the SiC patches, thus to stronger intermixing, which finally destroys the well-defined confinement of electrons in the SiC areas, as well as of the holes in the Ge dots. Consequently, the recombination probability drops.

In conclusion, we have demonstrated the Volmer-Weber growth of Ge dots on C precovered Si(001) surfaces by STM, caused by the surface strain fields related to the C-rich surface areas. The implications of this growth mode on further island development and the related PL mechanisms have been revealed.

*Email address: leifeld@mbe-components.com

¹O. Leifeld, R. Hartmann, B. Müller, E. Müller, K. Kern, and D. Grützmacher, *Appl. Phys. Lett.* **74**, 994 (1999).

²O.G. Schmidt, C. Lange, K. Eberl, O. Kienzle, and F. Ernst, *Appl. Phys. Lett.* **71**, 2340 (1997).

³O. Leifeld, D. Grützmacher, B. Müller, K. Kern, E. Kaxiras, and P. Kelires, *Phys. Rev. Lett.* **82**, 972 (1999).

⁴O. Leifeld, B. Müller, D. Grützmacher, and K. Kern, *Appl. Phys. A: Mater. Sci. Process.* **66**, S993 (1998).

⁵F. Liu and M.G. Lagally, *Phys. Rev. Lett.* **76**, 3156 (1996).

⁶Y.W. Mo, J. Kleiner, M.B. Webb, and M.G. Lagally, *Phys. Rev. Lett.* **66**, 1998 (1991).

⁷P.C. Kelires, *Int. J. Mod. Phys. C* **9**, 357 (1998).

⁸O. Leifeld, R. Hartmann, E. Müller, E. Kaxiras, K. Kern, and D. Grützmacher, *Nanotechnology* **10**, 122 (1999).

⁹Y.W. Mo and M.G. Lagally, *J. Cryst. Growth* **111**, 876 (1991).

¹⁰J.A. Venables, G.D.T. Spiller, and M. Hanbucken, *Rep. Prog. Phys.* **47**, 399 (1984).

¹¹O.G. Schmidt and K. Eberl, *Appl. Phys. Lett.* **73**, 2790 (1998).

¹²D. Grützmacher *et al.*, in *Proceedings of SPIE*, Vol. 3630, edited by D.C. Houghton and E.A. Fitzgerald (Society of Photo-Optical Instrumentation Engineers, Bellingham, WA, 1999), pp. 171–182.

¹³J. Weber and M.I. Alonso, *Phys. Rev. B* **40**, 5683 (1989).